1

Self-Cancellation of Sampling Frequency Offsets in STBC-OFDM Based Cooperative Transmissions

Zhen Gao[1] and Mary Ann Ingram[2]
[1]*Tsinghua University, Tsinghua Research Institute of Information Technology, Tsinghua National Laboratory for Information Science and Technology*
[2]*Georgia Institute of Technology*
[1]*P.R. China*
[2]*USA*

1. Introduction

Orthogonal frequency division multiplexing (OFDM) is a popular modulation technique for wireless communications (Heiskala & Terry, 2002; Nee & Prasad, 2000). Because OFDM is very effective for combating multi-path fading with low complex channel estimation and equalization in the frequency domain, the OFDM-based cooperative transmission (CT) with distributed space-time coding becomes a very promising approach for achieving spatial diversity for the group of single-antenna equipped devices (Shin et al., 2007; Li & Xia, 2007; Zhang, 2008; Li et al., 2010). Duo to the spacial diversity gain, CT is an energy efficient transmission technique, which can be used in sensor networks, cellular networks, or even satellite networks, to improve the communication quality or coverage.

However, OFDM systems are sensitive to sampling frequency offset (SFO), which may lead to severe performance degradation (Pollet, 1994). In OFDM based CTs, because the oscillator for DAC on each relay is independent, multiple SFOs exist at the receiver, which is a very difficult problem to cope with (Kleider et al., 2009). The common used correction method for single SFO is interpolation/decimation (or named re-sampling), which is a energy consuming procedure. And what is more important is that, because the re-sampling of the received signal can only correct single SFO, it seems helpless to multiple SFOs in the case of OFDM based CTs. Although the estimation of multiple SFOs in OFDM-based CT systems has been addressed by several researchers (Kleider et al., 2009; Morelli et al., 2010), few contributions have addressed the correction of multiple SFOs in OFDM-based CT systems so far to our knowledge. One related work is the tracking problem in MIMO-OFDM systems (Oberli, 2007), but it is assumed that all transmitting branches are driven by a common sampling clock, so there is still only one SFO at the receiver.

To provide an energy efficient solution to the synchronization problem of SFOs in OFDM based CTs, in Section 2 of this chapter, we firstly introduce a low-cost self-cancellation scheme that we have proposed for single SFO in conventional OFDM systems. Then we will show in the Section 3 that, the combination of the self-cancellation for single SFO and the re-

sampling method can solve the two SFOs problem in the two-branch STBC-OFDM based CTs. Simulations in the Section 4 will show that this low-cost scheme outperforms the ideal STBC system with no SFOs, and is robust to the mean SFO estimation error. In Section 5, the energy efficiency problem of the proposed schemes is analyzed. The chapter is summarized in Section 6.

2. SFO self-cancellation for conventional OFDM systems

The effect of SFO on the performance of OFDM systems was first addressed by T. Pollet (Pollet, 1994). SFO mainly introduces two problems in the frequency domain: inter-channel interference (ICI) and phase rotation of constellations. As mentioned in (Pollet, 1994; Speth et al., 1999; Pollet & Peeters, 1999; Kai et al., 2005) the power of the ICI is so small that the ICI are usually taken as additional noise. So the removal of SFO is mainly the correction of phase rotation.

Three methods have been proposed to correct single SFO. The first is to control the sampling frequency of the ADC directly at the receiver (Pollet & Peeters, 1999; Kim et al., 1998; Simoens et al., 2000). However, according to (Horlin & Bourdoux, 2008), this method does not suitable for low-cost analog front-ends. The second method is interpolation/ decimation (Speth et al., 1999; Kai et al. 2005; Speth et al., 2001; Fechtel, 2000; Sliskovic, 2001; Shafiee et al. 2004). The SFO is corrected by re-sampling the base-band signal in the time domain. The problem of this method is that the complexity is so high that it's very energy consuming for high-speed broadband applications. The third method is to rotate the constellations in the frequency domain (Pollet & Peeters, 1999; Kim et al. 1998;). The basis for this method is the delay-rotor property (Pollet & Peeters, 1999), which is that the SFO in the time domain causes phase shifts that are linearly proportional to the subcarrier index in the frequency domain. The performance of such method relies on the accuracy of SFO estimation. In previous works, there are three methods for SFO estimation. The first method is cyclic prefix (CP)-based estimation (Heaton, 2001). The performance of this method relies on the length of CP and the delay spread of the multipath channel. The second is the pilot-based method (Kim et al. 1998; Speth et al., 2001; Fechtel, 2000; Liu & Chong, 2002). The problem with this method is that, because the pilots are just a small portion of the symbol, it always takes several ten's of OFDM symbols for the tracking loop to converge. The third is the decision-directed (DD) method (Speth et al., 1999; Simoens et al., 2000). The problem of this method is that when SFO is large, the hard decisions are not reliable, so the decisions need to be obtained by decoding and re-constructing the symbol, which requires more memory and higher complexity. Because no estimation method is perfect, the correction method relying on the estimation will not be perfect.

Based on above considerations, we proposed a low-cost SFO self-cancellation scheme for conventional OFDM systems in (Gao & Ingram, 2010). In this section, we give a brief introduction of the self-cancellation scheme for single SFO, and then Section 3 will show how this scheme can be applied for the problem of two SFOs in STBC-OFDM based CTs.

Instead of focusing on the linearity between phase shifts caused by SFO and subcarrier index as usual, the scheme in (Gao & Ingram, 2010) makes use of the symmetry property of the phase shifts. By putting the same constellation on symmetrical subcarrier pairs, and combining the pair coherently at the receiver, the phase shifts caused by SFO on

symmetrical subcarriers approximately cancel each other. Considering that the residual CFO may exist in the signal, pilots are also inserted symmetrically in each OFDM symbol, so that the phase tracking for residual CFO can work as usual. Although it can be expected that, because no SFO estimation and correction processing are needed, the complexity and energy consuming of the SFO self-cancellation should be very low, this aspect is not considered carefully in (Gao & Ingram, 2010). So in this chapter, a detailed discussion about the complexity problem for the proposed scheme is provided in Section 5.

2.1 Signal model

The FFT length (or number of subcarriers) is N, in which N_d subcarriers are used for data symbols and N_p subcarriers are used for pilot symbols. The length of CP is N_g, so the total length of one OFDM symbol is $N_s = N + N_g$. f_s denotes the sampling frequency of the receiver, and $T_s = 1/f_s$ is the sample duration at the receiver. We assume the symbol on the k-th subcarrier is a_k, H_k is the channel response on the k-th subcarrier, Δf is the residual CFO normalized by the subcarrier spacing, and $\varepsilon = (T_{s\text{-}tx} - T_s)/T_s$ is the SFO, where $T_{s\text{-}tx}$ is the sample duration at the transmitter. Then the transmitted signal in the time domain can be expressed as

$$x_n = \frac{1}{N}\sum_{k=-N/2}^{N/2-1} a_k e^{j2\pi nk/N},\ n = 0,1,...N-1. \tag{1}$$

After passing through the physical channel h_l and corrupted by the residual CFO Δf and SFO ε, the complex envelope of the received signal without noise can be expressed as

$$\begin{aligned} r_n &= e^{j2\pi\Delta fn/N}\left(h_l * x_n\right) \\ &= e^{j2\pi\Delta fn/N}\frac{1}{N}\sum_{k=-N/2}^{N/2-1} a_k H_k e^{j2\pi n(1+\varepsilon)k/N}. \end{aligned} \tag{2}$$

After removing the CP and performing DFT to r_n, the symbol in the frequency domain can be expressed as (Zhao & Haggman, 2001)

$$\begin{aligned} z_k &= \sum_{n=0}^{N-1} r_n e^{-j2\pi kn/N} \\ &= \sum_{n=0}^{N-1}\left[e^{j2\pi\Delta fn/N}\frac{1}{N}\sum_{k=-N/2}^{N/2-1} X_k H_k e^{j2\pi n(1+\varepsilon)k/N}\right]e^{-j2\pi kn/N}, \\ &= a_k H_k S(\Delta f + \varepsilon k) + \sum_{\substack{l=-N/2 \\ l\neq k}}^{N/2-1} a_l H_l S(\Delta f + \varepsilon l + l - k) \end{aligned} \tag{3}$$

where $S(x) = \dfrac{\sin[\pi x]}{N\sin[\pi x/N]} e^{j\pi x(N_s+N_g-1)/N}$.

Now, if the constellation transmitted on the k-th subcarrier of the m-th OFDM symbol and the corresponding noise are $a_{m,k}$ and $w_{m,k}$, respectively, the received symbol in the frequency domain can be easily got from (3) as

$$z_{m,k} = (e^{j\pi\phi_k} e^{j2\pi((mN_s+N_g)/N)\phi_k})\mathrm{sinc}(\pi\phi_k)a_{m,k}H_k + w_{ICI,k} + w_{m,k}\,, \tag{4}$$

where $\phi_k \approx \Delta f + \varepsilon k$, $\mathrm{sinc}(\pi\phi_k) = \dfrac{\sin\pi\phi_k}{N\sin(\pi\phi_k/N)}$ and $w_{ICI,k} = \sum_{\substack{l=-N/2 \\ l\neq k}}^{N/2-1} a_l H_l S(\Delta f + \varepsilon l + l - k)$ is the ICIs from all other subcarriers.

In (4), $e^{j\pi\phi_k}$ and $\mathrm{sinc}(\pi\phi_k)$ are the local phase increment and local amplitude gain, respectively. They will be combined into the estimated channel response as $H_k' = e^{j\pi\phi_k}\mathrm{sinc}(\pi\phi_k)H_k$. So, after channel equalization, (4) becomes

$$z_{m,k} = e^{j2\pi((mN_s+N_g)/N)\phi_k} a_{m,k} + w'_{ICI,k} + w'_{m,k}\,, \tag{5}$$

where $w'_{ICI,k} = w_{ICI,k} / H_k'$ and $w'_{m,k} = w_{m,k} / H_k'$. In (5), only the accumulated phase $e^{j2\pi((mN_s+N_g)/N)\phi_k}$ needs to be corrected.

2.2 The idea of SFO self-cancellation scheme

The SFO self-cancellation scheme is inspired by the relationship between phase shifts and the subcarrier index. Fig. 1 is a simulation result that demonstrates the phase shifts caused

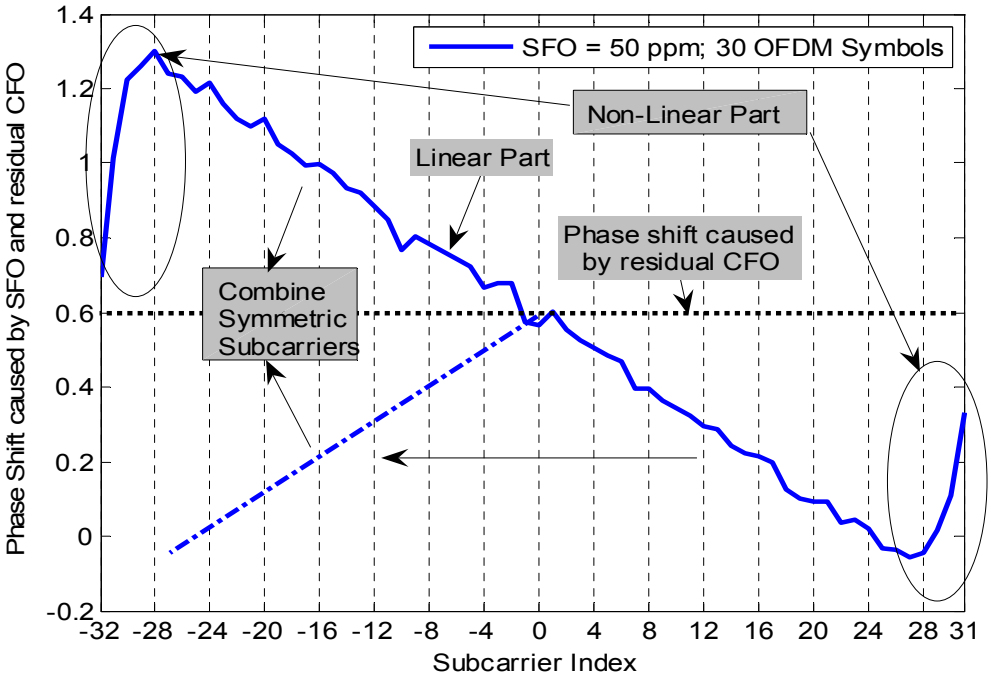

Fig. 1. Linearity and Symmetry of the Phase Shifts caused by SFO

by residual CFO and SFO. The figure shows two phenomenons. The first is that the phase shifts for the subcarriers in the middle are linearly proportional to the subcarrier index. This is the delay-rotor property mentioned above, and has been explored a lot for estimation and correction of SFO. Note that the phase shifts for the edge subcarriers do not obey the linearity. In practice, for the convenience of design of transmit and receive filters, and inter-channel interference suppression, these subcarriers are usually set to be zeros (IEEE, 1999). The other fact is that the phase shifts caused by SFO are symmetrical relative to the common phase shift caused by residual CFO (dotted horizontal line in Fig. 1). So if we put the same constellation on symmetrical subcarriers, we may be able to combine the symbols at the receiver in a way such that the phase shifts on these two subcarriers caused by SFO can approximately cancel each other. This mapping can be called "Symmetric Symbol Repetition (SSR)", which is different from other self-cancellation techniques, such as "Adjacent Symbol Repetition (ASR)" (Zhao & Haggman, 2001), "Adjacent Conjugate Symbol Repetition (ACSR)" (Sathananthan, 2004), and "Symmetric Conjugate Symbol Repetition (SCSR)" (Tang, 2007). It should be pointed out that the self-cancellation of the phase shifts caused by SFO on symmetric subcarrier cannot be achieved by other repetition schems. Taking SCSR as an example, the addition of conjugate symbols on symmetric subcarriers also removes the phase of the symbols, which makes the symbol undetectable.

2.3 Analysis of the SFO self-cancellation scheme

Assuming the same constellation $a_{m,k}$ is mapped on symmetrical subcarriers $-k$ and k of the m-th OFDM symbol, the signal on the pair of subcarriers after channel equalization can be expressed as (according to (5))

$$\begin{cases} z_{m,k} = e^{jF_m\phi_k} a_{m,k} + w'_{ICI,k} + w'_{m,k} \\ z_{m,-k} = e^{jF_m\phi_{-k}} a_{m,k} + w'_{ICI,-k} + w'_{m,-k} \end{cases}, \tag{6}$$

where $F_m = 2\pi((mN_s + N_g)/N)$. Then the combination of $z_{m,k}$ and $z_{m,-k}$ is

$$z'_{m,k} = 2\cos(F_m\varepsilon k)e^{jF_m\Delta f} a_{m,k} + \alpha w'_{ICI,k} + w''_{m,k}. \tag{7}$$

We see that the phase shifts introduced by SFO is removed, and the residual phase $e^{jF_m\Delta f}$ is a common term, which can be corrected by phase tracking. Because $F_m\varepsilon k$ <<1, $2\cos(F_m\varepsilon k) \approx 2$. In other words, the two subcarriers are combined coherently. In addition, because the energy of ICIs is mainly from residual CFO, and the ICIs caused by residual CFO are same for symmetrical subcarriers, the ICIs on symmetrical subcarriers are also combined almost coherently, which means $a \approx 2$. So the average SIR does not change after combination. $w'_{m,k}$ and $w'_{m,-k}$ are independent, so the final noise term is

$$w''_{m,k} = w'_{m,k} + w'_{m,-k} = w_{m,k}/H_k' + w_{m,-k}/H_{-k}'. \tag{8}$$

Assuming $E\{|a_{m,k}|^2\} = 1$, $E\{|H_k|^2\} = 1$, $E\{|w_{ICI,k}|^2\} = \sigma_{ICI}^2$, and $E\{|w_{m,k}|^2\} = \sigma_n^2$, under the assumption that $\sigma_{ICI}^2 << \sigma_n^2$, the average $SINR$ before combination (see (5)) and after combination (see (7)) are

$$\begin{cases} SINR_{Bf} = \dfrac{1}{\sigma_{ICI}^{\ 2} + \sigma_n^{\ 2}} \approx \dfrac{1}{\sigma_n^{\ 2}} \\ SINR_{Af} \approx \dfrac{4}{4\sigma_{ICI}^{\ 2} + 2\sigma_n^{\ 2}} \approx \dfrac{2}{\sigma_n^{\ 2}} \end{cases} . \tag{9}$$

So the average SINR has been improved by 3dB, which is the array gain from the combination. In addition, because small values are more likely to get for $2|H_k'|^2$ than for $(1/|H_k'|^2+1/|H_{-k}'|^2)^{-1}$, some diversity gain is achieved. Fig. 2 shows that this diversity gain is smaller that of the 2-branch MRC. In the figure, H1, H2 and H are independent Rayleigh fading random variables.

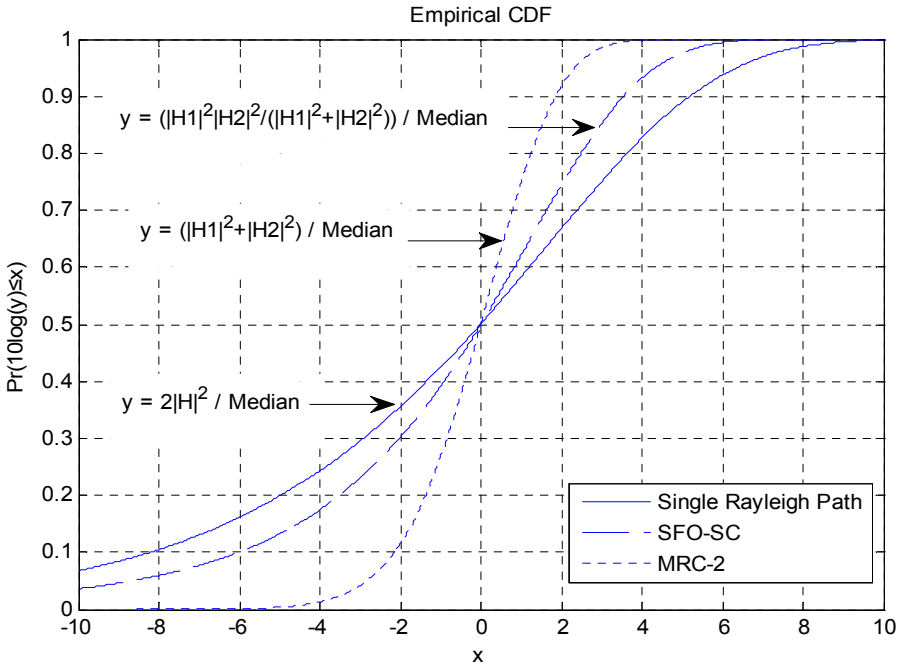

Fig. 2. Diversity gain from Symmetric Combination

2.4 System structure

Fig. 3 gives the structure of the transmitter and receiver with the SFO self-cancellation scheme. At the transmitter, the "Modulation on Half Subcarriers" and "Symmetrical Mapping" blocks compose the "Self-Cancellation Encoding" module. At the receiver, the "Channel Equalization" and "Symmetrical Combining" blocks compose the "Self-Cancellation Decoding" module. For the coarse CFO synchronization and channel estimation, repeated short training blocks and repeated long training blocks compose the preamble. To remove the residual CFO, the phase shifts on pilots after the SFO self-cancellation decoding are averaged to get one phase shift, which is multiplied to all the data subcarriers after the self-cancellation decoding.

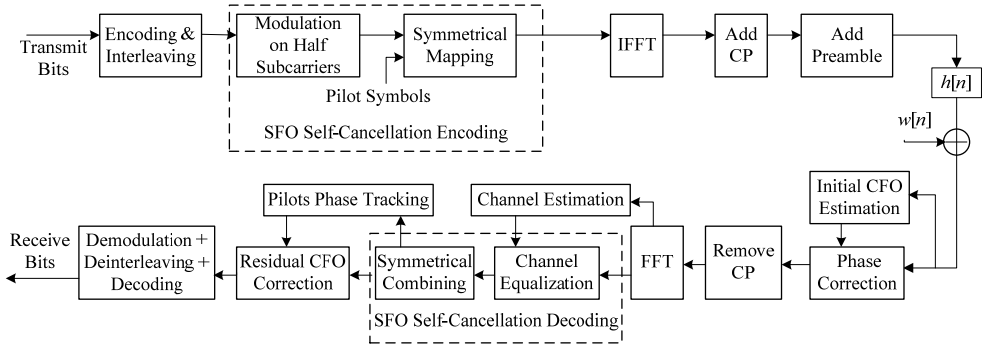

Fig. 3. Block diagram of the Transmitter and Receiver with the SFO Self-Cancellation Scheme

Fig. 4 shows how to do the symmetrical mapping. For the purpose of phase tracking for residual CFO correction, pilot symbols are also mapped symmetrically. For the convenient of design of transmit filter and receive filter, the subcarriers on the edge are set to be zeros.

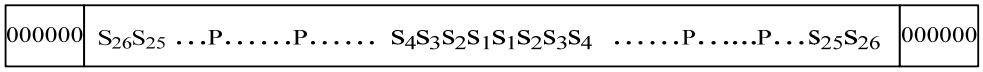

Fig. 4. Symmetrical Mapping

3. SFOs self-cancellation scheme for Alamouti coded OFDM based CTs

In this section, we propose a self-cancellation scheme for the two SFOs in the 2-branch Alamouti coded OFDM based CT systems. The scheme is the combination of the SFO self-cancellation scheme introduced in Section 2 and the re-sampling method, which is the conventional method for single SFO compensation.

3.1 Alamouti coded OFDM based cooperative transmission

We consider a commonly used cooperative system model (Fig. 5), which includes one source, one relay and one destination. Every node is equipped with one antenna. This structure is a very popular choice for coverage increase in sensor networks and for quality improvement for uplink transmissions in cellular networks (Shin et al., 2007). The communication includes two phases. In Phase 1, the source broadcasts the message to the relay and the destination. We assume the relay can decode the message correctly. Then, both the relay and the source will do 2-branch STBC-OFDM encoding according to Alamouti scheme (Alamouti, 1998). In Phase 2, the source transmits one column of the STBC matrix to the destination, and the relay transmits the other column. In Fig. 5, (f_1, T_1), (f_2, T_2), (f_d, T_d) are the carrier frequency and sample duration of the source, relay and the destination, respectively. This structure is well studied by (Shin, 2007). In this section, we assume timing synchronization and coarse carrier frequency synchronization have been performed according to (Shin, 2007), so only residual CFOs and SFOs exist in the received signal at the destination.

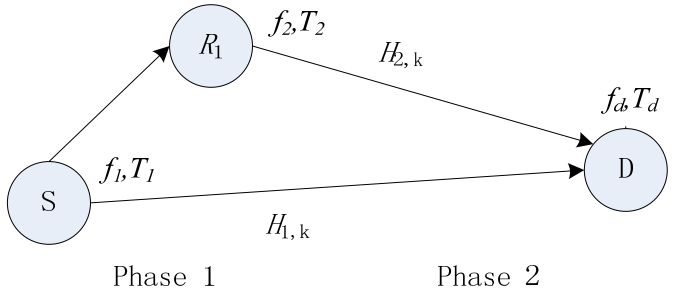

Fig. 5. Cooperative Transmission Architecture

3.2 Effect of residual CFOs and SFOs in Alamouti coded signals

According to the Alamouti scheme (Alamouti, 1998), the transmitted signal matrix for the k-th subcarrier by the source and the relay in two successive OFDM symbols is

$$\begin{bmatrix} a_{m,k} & -a_{m+1,k}^{*} \\ a_{m+1,k} & a_{m,k}^{*} \end{bmatrix}.$$

The first column is for the m-th OFDM symbol duration and the second column is for the (m+1)-th OFDM symbol duration. If there are no CFOs and SFOs, the received signals on the k-th subcarrier of successive OFDM symbols are

$$\begin{cases} z_{m,k} = a_{m,k}H_{1,k} + a_{m+1,k}H_{2,k} + w_{m,k} \\ z_{m+1,k} = -a_{m+1,k}^{*}H_{1,k} + a_{m,k}^{*}H_{2,k} + w_{m,k+1} \end{cases}, \tag{10}$$

where $H_{t,k}$ (t = 1, 2) is the frequency domain response of the channels between two transmitters and the destination. We assume the channels are static during the transmission of one packet.

If the residual CFOs and SFOs between the two transmitters and the destination are (Δf_1, ε_1) and (Δf_2, ε_2), following the procedure in Section 2.1, the received OFDM symbols at the destination become

$$\begin{aligned} z_{m,k} = {} & a_{m,k}e^{j\pi\phi_{1,k}}e^{jF_m\phi_{1,k}}\mathrm{sinc}(\phi_{1,k})H_{1,k} + a_{m+1,k}e^{j\pi\phi_{2,k}}e^{jF_m\phi_{2,k}}\mathrm{sinc}(\phi_{2,k})H_{2,k} \\ & + w_{m,ICI} + w_{m,k} \end{aligned}, \tag{11}$$

and

$$\begin{aligned} z_{m+1,k} = {} & -a_{m+1,k}^{*}e^{j\pi\phi_{1,k}}e^{jF_{m+1}\phi_{1,k}}\mathrm{sinc}(\phi_{1,k})H_{1,k} + a_{m,k}^{*}e^{j\pi\phi_{2,k}}e^{jF_{m+1}\phi_{2,k}}\mathrm{sinc}(\phi_{2,k})H_{2,k} \\ & + w_{m+1,ICI} + w_{m+1,k} \end{aligned}, \tag{12}$$

in which $\phi_{t,k} = \Delta f_t + \varepsilon_t k$, and $w_{m,ICI}$ and $w_{m+1,ICI}$ are the ICIs caused by residual CFOs and SFOs. Because the power of ICI is very small, $w_{m,ICI}$ and $w_{m+1,ICI}$ are usually taken as

additional noise. So we can define $w'_{m,k} = w_{m,ICI} + w_{m,k}$ and $w'_{m+1,k} = w_{m+1,ICI} + w_{m+1,k}$ as the effective noise.

In (11) and (12), $e^{j\pi\phi_{t,k}}$ and $\mathrm{sinc}(\pi\phi_{t,k})$ are the local phase increment and local amplitude attenuation caused by the residual CFOs and SFOs, respectively, and they are usually combined into the estimated channel responses as $H'_{t,k} = e^{j\pi\phi_{t,k}}\mathrm{sinc}(\pi\phi_{t,k})H_{t,k}$. Before STBC decoding, these two estimated channels are corrected through phase tracking based on pilot symbols (Shin, 2007). In this section, we assume the channel estimations and phase tracking for residual CFOs are perfect, so that we can focus on the effect of SFOs. If $\varphi_t = F_m\Delta f_t$ and $\theta_{t,k} = F_m\varepsilon_t k$, the channel responses after phase correction becomes $H''_{t,k} = e^{j\pi\varphi_t}e^{j\pi\phi_{t,k}}\mathrm{sinc}(\pi\phi_{t,k})H_{t,k}$. Then the STBC decoded symbols are

$$\begin{aligned}\hat{a}_{m,k} &= (H''^{*}_{1,k} z_{m,k} + H''_{2,k} z^{*}_{m+1,k}) / (|H''_{1,k}|^2 + |H''_{2,k}|^2) \\ &= \frac{(a_{m,k}e^{j\theta_{1,k}}|H''_{1,k}|^2 + a_{m,k}e^{-j\theta_{2,k}}|H''_{2,k}|^2 + a_{m+1,k}e^{j\theta_{2,k}}H''_{2,k}H''^{*}_{1,k} - a_{m+1,k}e^{-j\theta_{1,k}}H''_{2,k}H''^{*}_{1,k})}{(|H''_{1,k}|^2 + |H''_{2,k}|^2)} \\ &\quad + (H''^{*}_{1,k} w'_{m,k} + H''_{2,k} w'^{*}_{m+1,k}) / (|H''_{1,k}|^2 + |H''_{2,k}|^2)\end{aligned} \tag{13}$$

and

$$\begin{aligned}\hat{a}_{m+1,k} &= (H''^{*}_{2,k} z_{m,k} - H''_{1,k} z^{*}_{m+1,k}) / (|H''_{1,k}|^2 + |H''_{2,k}|^2) \\ &\approx \frac{(a_{m+1,k}e^{j\theta_{2,k}}|H''_{2,k}|^2 + a_{m+1,k}e^{-j\theta_{1,k}}|H''_{1,k}|^2 + a_{m,k}e^{j\theta_{1,k}}H''^{*}_{2,k}H''_{1,k} - a_{m,k}e^{-j\theta_{2,k}}H''^{*}_{2,k}H''_{1,k})}{(|H''_{1,k}|^2 + |H''_{2,k}|^2)}, \\ &\quad + (H''^{*}_{1,k} w'_{m,k} - H''_{2,k} w'^{*}_{m+1,k}) / (|H''_{1,k}|^2 + |H''_{2,k}|^2)\end{aligned} \tag{14}$$

where we apply the approximation $F_m \approx F_{m+1}$ in (14). From (13) and (14) we see that, the SFOs destroy the orthogonality of the two STBC branches, so the symbols cannot be recovered perfectly by STBC decoding.

3.3 SFOs self-cancellation

If we apply the SFO self-cancellation scheme for single SFO directly into STBC decoded signals, the symbol on the *k*-th subcarrier after symmetrical combination becomes

$$\begin{aligned}\hat{a}'_{m,k} &= \hat{a}_{m,k} + \hat{a}_{m,-k} \\ &= \frac{a_{m,k}e^{j\theta_{1,k}}|H''_{1,k}|^2 + a_{m,k}e^{-j\theta_{2,k}}|H''_{2,k}|^2}{|H''_{1,k}|^2 + |H''_{2,k}|^2} + \frac{a_{m,k}e^{-j\theta_{1,k}}|H''_{1,-k}|^2 + a_{m,k}e^{j\theta_{2,k}}|H''_{2,-k}|^2}{|H''_{1,-k}|^2 + |H''_{2,-k}|^2} \\ &\quad + \frac{a_{m+1,k}e^{j\theta_{2,k}}H''_{2,k}H''^{*}_{1,k} - a_{m+1,k}e^{-j\theta_{1,k}}H''_{2,k}H''^{*}_{1,k}}{|H''_{1,k}|^2 + |H''_{2,k}|^2} + \frac{a_{m+1,k}e^{-j\theta_{2,k}}H''_{2,-k}H''^{*}_{1,-k} - a_{m+1,-k}e^{j\theta_{1,k}}H''_{2,-k}H''^{*}_{1,-k}}{|H''_{1,-k}|^2 + |H''_{2,-k}|^2}, \\ &\quad + \frac{H''^{*}_{1,k} w'_{m,k} + H''_{2,k} w'^{*}_{m+1,k}}{|H''_{1,k}|^2 + |H''_{2,k}|^2} + \frac{H''^{*}_{1,-k} w'_{m,-k} + H''_{2,-k} w'^{*}_{m+1,-k}}{|H''_{1,-k}|^2 + |H''_{2,-k}|^2}\end{aligned} \tag{15}$$

By examining the structure of (15) carefully, we find that if $\theta_{1,k} = -\theta_{2,k} = \theta_k$, or equivalently $\varepsilon_1 = -\varepsilon_2 = \varepsilon$, the interference term (the second line of (15)) becomes zero, and then we can have

$$\hat{a}'_{m,k} = G_{m,k} a_{m,k} + w''_{m,k}, \tag{16}$$

where we define

$$G_{m,k} = 2\cos(F_m \varepsilon k) \text{ and } w''_{m,k} = \frac{H''^{*}_{1,k} w'_{m,k} + H''_{2,k} w'^{*}_{m+1,k}}{\left|H''_{1,k}\right|^2 + \left|H''_{2,k}\right|^2} + \frac{H''^{*}_{1,-k} w'_{m,-k} + H''_{2,-k} w'^{*}_{m+1,-k}}{\left|H''_{1,-k}\right|^2 + \left|H''_{2,-k}\right|^2}.$$

From (16), we see that if we can make $\varepsilon_1 = -\varepsilon_2 = \varepsilon$, the phase shifts and interferences caused by SFOs can be completely removed, and the symbols can be detected successively. Fortunately, interpolation/decimation, or re-sampling, can help us to achieve this goal. Firstly, the receiver need to estimate the mean value of the two SFOs, and then adjust sampling frequency to the average of the two transmit sampling frequencies through re-sampling, which makes the two residual SFOs opposite. The discussion about the mean SFO estimation is given in Section 3.5, and simulations in Section 4 will show the robustness of our design to the mean SFO estimation error.

Fig. 6 describes a complete system structure with the SFOs self-cancellation scheme for Alamouti coded OFDM based CT. During the cooperation phase, SSR and Alamouti encoding are performed at the source and the relay. Then, the source transmits one column of the STBC matrix to the destination, and the relay transmits the other one. The preamble at the beginning of the packet includes the training for timing synchronization, initial CFO estimation, channel estimation, and mean SFO estimation. The estimated mean SFO is then used to adjust the sampling frequency through interpolation/decimation. This adjustment makes the residual SFOs in two branches opposite, which makes the STBC decoded symbols have the form of (16). Finally, the SFO self-cancellation decoding performs symmetrical combination to remove the effect of SFO in each orthogonal branch.

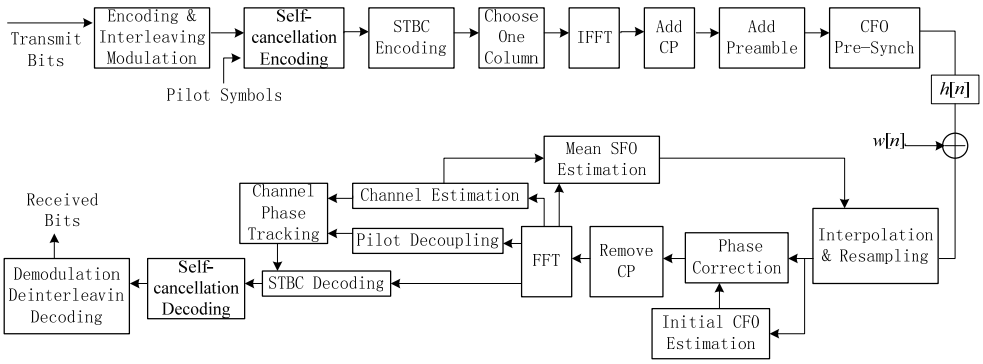

Fig. 6. Block diagram of the Self-Cancellation Scheme in Alamouti Coded OFDM based CTs

3.4 Analysis of diversity gain and array gain

Based on (16), the SNR after the SFO self-cancellation decoding can be calculated as

$$\frac{S_{stbc\text{-}sc}}{N_{stbc\text{-}sc}} = \frac{G_{m,k}{}^2 \rho}{\sigma_w{}^2}\left(\frac{1}{\left|H_{1,k}''\right|^2 + \left|H_{2,k}''\right|^2} + \frac{1}{\left|H_{1,-k}''\right|^2 + \left|H_{2,-k}''\right|^2}\right)^{-1}.$$

So the SNR gain can be expressed as

$$G_{snr} = \frac{S_{stbc\text{-}sc}}{N_{stbc\text{-}sc}} \Big/ \frac{\rho}{\sigma_w{}^2} = G_a G_d ,$$

where we define

$$G_a = \frac{G_{m,k}{}^2}{2} \text{ and } G_d = 2\left(\frac{1}{\left|H_{1,k}''\right|^2 + \left|H_{2,k}''\right|^2} + \frac{1}{\left|H_{1,-k}''\right|^2 + \left|H_{2,-k}''\right|^2}\right)^{-1}$$

as the array gain and diversity gain, respectively. Because $F_m \varepsilon k << 1$, the array gain is a little bit smaller than 2. This gain comes from the fact that we combine the useful signals coherently, but the noise terms are added non-coherently. Fig. 7 plots G_d together with the CDF of standard Rayleigh and MRC of two Rayleigh random variables for normal STBC. We see that, in addition to the diversity gain from STBC, we get extra diversity gain from

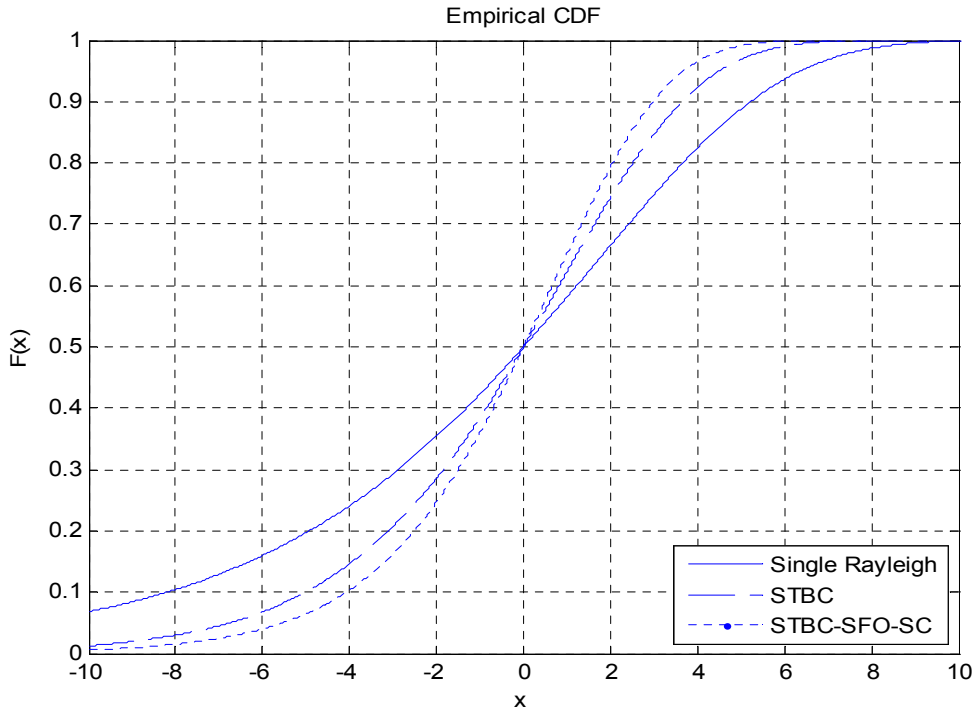

Fig. 7. Diversity Gain of STBC-SC

the SFO self-cancellation scheme. This is because the symmetrical combination actually averages the channels on symmetrical subcarriers, which makes the equivalent channel "flatter".

3.5 Discussion about the mean SFO estimation

There are two choices for the mean SFO estimation. One is to estimate the mean SFO directly, and the other is to estimate two SFOs separately and then get the mean value of the estimates. For direct estimation, two relays may transmit common training blocks, and the receiver does the SFO estimation based on the training using conventional SFO estimation method for single SFO. In this case, estimation result should be some kind of weighted average of the two SFOs, not exact the mean SFO. The second choice should be unbiased, but special training structure needs to be designed for the separate estimation. As mentioned in (Morelli, 2010), for the ML estimator of residual CFO and SFO, the two parameters are coupled, so the ML solution involves a 2-dimensional grid-search, which is difficult to pursue in practice. On the other hand, if we still need to estimate the two SFOs accurately, the self-cancellation scheme is not so valuable. So our comment is that, in the CT systems applying our SFOs self-cancellation schemes, the simple direct estimation of the mean SFO is favorable. Although the accuracy of this method may not be very high, the simulations in Section 4 will show that the self-cancellation scheme is robust to the estimation error. In addition, similar to the single SFO estimation for conventional OFDM systems, a PI (proportional-integral) tracking loop can be used to improve the accuracy of the mean SFO estimation (Speth et al., 2001).

4. Simulations

Simulations are run to examine the performance of our SFOs self-cancellation scheme in the STBC-OFDM based cooperative transmissions. In the simulation, N = 64, N_g = 16, N_s = 80, and one packet contains 50 OFDM symbols. No channel coding is applied in the simulations. The typical urban channel model COST207 (Commission of the European Communities, 1989) is used, and the channel power is normalized to be unity. We assume the difference between two SFOs is 100 *ppm*. If the mean SFO estimation is perfect, the residual SFO should be SFO1/SFO2 = 50/-50ppm. Because the mean SFO estimation may not be perfect, the phase shifts and interferences may still exist in the decoded signals. In following simulations, we firstly examine the effect of the mean SFO estimation error to the residual phase shifts and signal to interference radio (SIR) in both normal STBC and STBC with SFO self-cancellation (STBC-SC). And then we show the overall effect of SFOs to the constellations. Finally, we compare the BER performance of STBC and STBC-SC when two SFOs exist.

4.1 Residual phase shifts

Fig. 8 shows the residual phase after STBC decoding and SFO self-cancellation decoding for different SFO1/SFO2. For STBC, the residual phase is measured as $E\left[\angle \hat{a}_{m,k} a_{m,k}^{*}\right]$ (see (13)), and for STBC-SC, it is measured as $E\left[\angle \hat{a}'_{m,k} a_{m,k}^{*}\right]$ (see (15)). In the simulation, the value of SFO1 changes gradually from 0 to 100 *ppm*, and SFO2 changes correspondingly as SFO1 – 100 (*ppm*). Because the phase shifts are different for different subcarriers in different OFDM

symbols, the 13th (k=13) and 26th (k=26) subcarriers in the 50th OFDM symbol (m = 50) are chosen as examples. Fig. 8 shows that the residual phase is reduced significantly by the symmetrical combination. The residual phase for STBC (circle lines) is only determined by the difference of the two SFOs (100ppm), and not very related to the value of SFO1 and SFO2. But for SFO self-cancellation (dot lines), when SFO1 = -SFO2, the residual phase is 0, and the larger is the mean SFO estimation error, the larger is the residual phase. For the 13th subcarrier, the increase of the residual phase is very small, so we can say the residual phase of STBC-SC is not sensitive to the mean SFO estimation error on average.

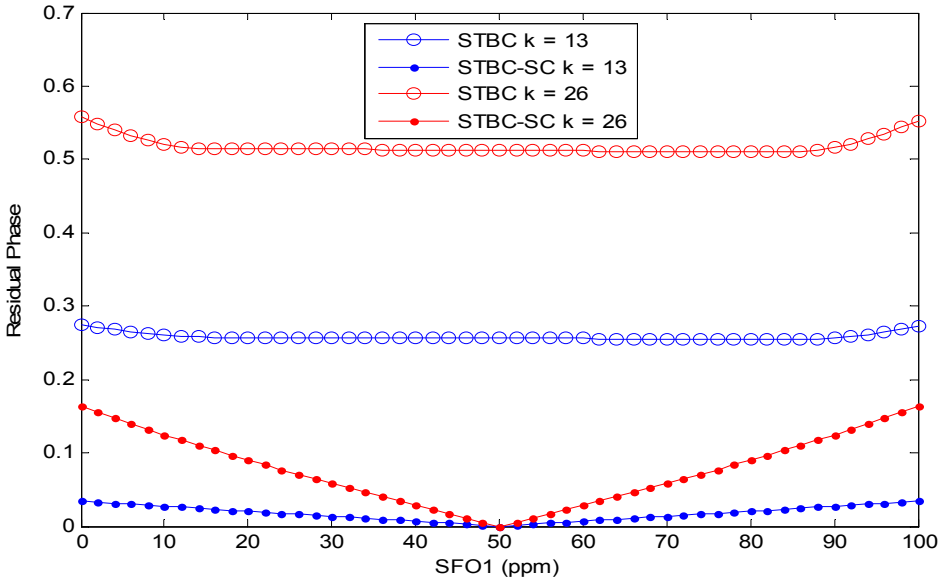

Fig. 8. Residual Phase (k=13/26, m=50)

4.2 SIR

When SFO1 ≠ -SFO2, interferences come out in the decoded symbols, and destroy the orthogonality of the STBC structure. Fig. 9 shows the SIR for STBC and STBC-SC for different SFO1/ SFO2. Based on (13) and (15), the SIR for STBC and STBC-SC are calculated as

$$\begin{cases} SIR_{stbc} = \dfrac{E\left[\left|a_{m,k}e^{j\theta_{1,k}}\left|H''_{1,k}\right|^2 + a_{m,k}e^{-j\theta_{2,k}}\left|H''_{2,k}\right|^2\right|^2\right]}{E\left[\left|a_{m+1,k}e^{j\theta_{2,k}}H''_{2,k}H''^{\,*}_{1,k} - a_{m+1,k}e^{-j\theta_{1,k}}H''_{2,k}H''^{\,*}_{1,k}\right|^2\right]} \\ SIR_{stbc-sc} = \dfrac{E\left[\left|\dfrac{a_{m,k}e^{j\theta_{1,k}}\left|H''_{1,k}\right|^2 + a_{m,k}e^{-j\theta_{2,k}}\left|H''_{2,k}\right|^2}{\left|H''_{1,k}\right|^2 + \left|H''_{2,k}\right|^2} + \dfrac{a_{m,k}e^{-j\theta_{1,k}}\left|H''_{1,-k}\right|^2 + a_{m,k}e^{j\theta_{2,k}}\left|H''_{2,-k}\right|^2}{\left|H''_{1,-k}\right|^2 + \left|H''_{2,-k}\right|^2}\right|^2\right]}{E\left[\left|\dfrac{a_{m+1,k}e^{j\theta_{2,k}}H''_{2,k}H''^{\,*}_{1,k} - a_{m+1,k}e^{-j\theta_{1,k}}H''_{2,k}H''^{\,*}_{1,k}}{\left|H''_{1,k}\right|^2 + \left|H''_{2,k}\right|^2} + \dfrac{a_{m+1,k}e^{j\theta_{2,k}}H''_{2,-k}H''^{\,*}_{1,-k} - a_{m+1,-k}e^{j\theta_{1,k}}H''_{2,-k}H''^{\,*}_{1,-k}}{\left|H''_{1,-k}\right|^2 + \left|H''_{2,-k}\right|^2}\right|^2\right]} \end{cases}$$

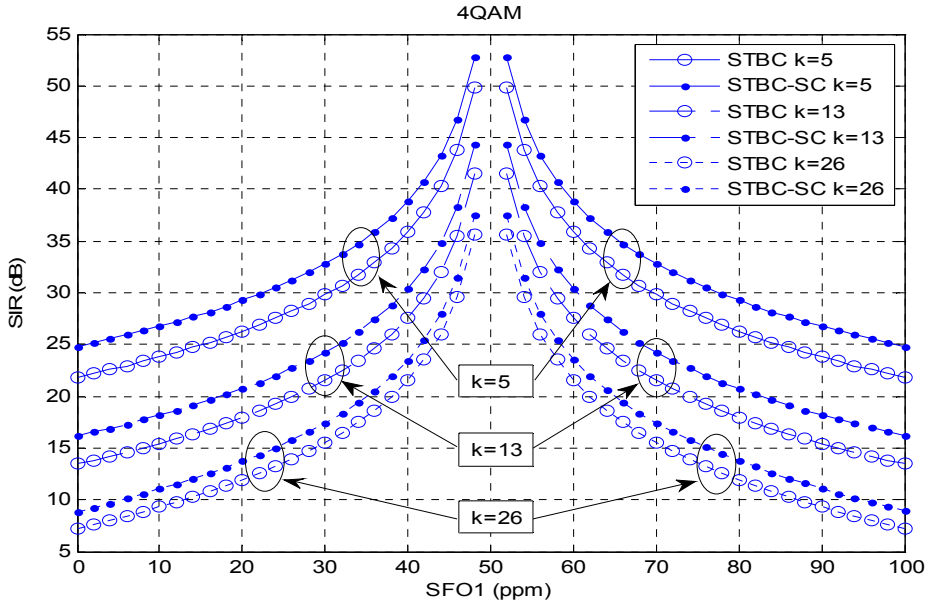

Fig. 9. SIR for Different SFO1/SFO2 (k=5/13/26, m=50)

We choose k = 5/13/26 and m = 50. We see that, for both STBC and STBC-SC, the larger is the mean SFO estimation error, the lower is the SIR. From (15), we can see that, in the symmetrical combination, useful signals are combined coherently, and the interferences are combined non-coherently. So the SIR for STBC-SC is about 3dB larger than that for STBC. When k is large, because the amplitude gain for STBC-SC, $G_{m,k}$ in equation (16), is obviously smaller than 2, the SIR improvement is smaller than 3dB (e.g. about 2dB for k = 26). Fig. 10 shows the SIR for the positive half part of the subcarriers when the mean SFO estimation is 20ppm (SFO1/SFO2 = 70/-30ppm). It's clear that the closer is the subcarrier to the center (k = 0), the larger is the SIR. Also, for small k, the improvement of SFO self-cancellation is about 3dB over STBC, but this improvement decreases for larger k.

4.3 Effect of SFOs to the constellations

Fig. 11 shows the effect of the SFOs to the decoded symbols in one packet for STBC and STBC-SC. No noise is added in the simulation. When there is no mean SFO estimation error (SFO1/SFO2 = 50/-50ppm, Fig. 11 (a)), there is no interference, so the effect of SFOs to STBC decoded symbols is just spreading one constellation point to a "strip", which effect is removed by the symmetrical combination in STBC-SC. When the mean SFO estimation error is 20ppm (SFO1/SFO2 = 70/-30ppm, Fig. 11 (b)), for STBC, the interferences are obvious for the points at the edges of the "phase spread strip", and much less obvious for the points in the middle of the strip. The reason is that, the points at the edges of the strip correspond to the symbols on the edge (e.g. k = ±25 or ±26). From Fig. 10 we know that the SIRs for these subcarriers are low, so the interferences are obvious. For STBC-SC, because the phase spread is mitigated, the influence range of the interferences is much smaller than that for STBC.

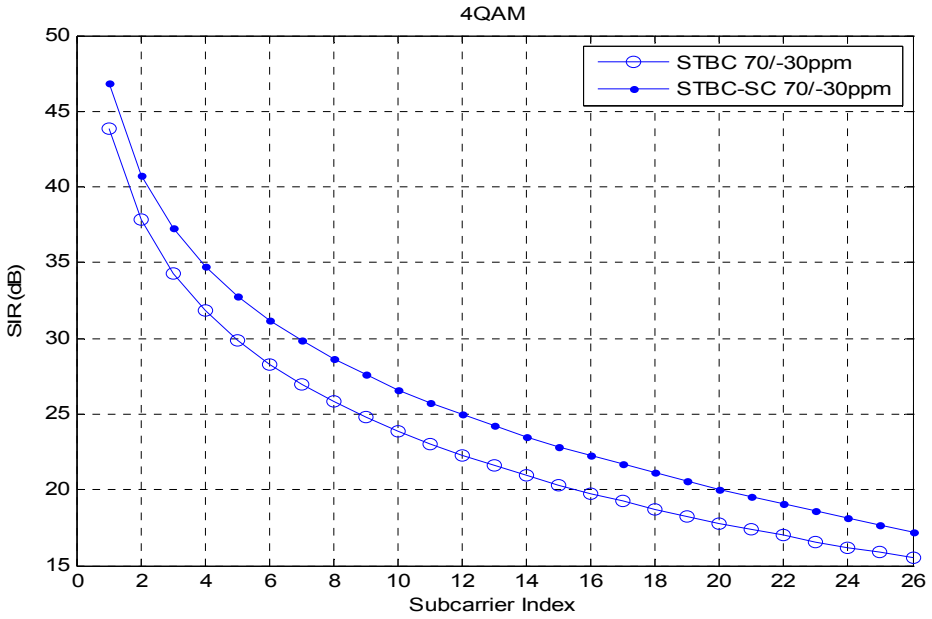

Fig. 10. SIR for Different subcarriers

4.4 BER performance

Fig. 12 shows the effect of SFOs to the BER performance of STBC and STBC-SC when QPSK is used. When SFO1/SFO2 = 50/-50ppm, STBC-SC outperforms STBC by about 5dB. When the mean SFO estimation error is 20ppm (SFO1/SFO2 = 70/-30ppm), the degradation of STBC for BER = 4×10^{-5} is more than 3dB, but the degradation of STBC-SC is less than 1dB. So we can say STBC-SC is robust to the mean SFO estimation error. The BER for STBC with no SFOs is also given as a reference (the triangle-dashed curve). We see that STBC-SC outperforms the ideal STBC by about 4dB when BER = 10^{-4}. Part of the improvement comes from the array gain and diversity gain brought by the symmetrical combination. But the more important reason is that, as shown in Fig. 11, STBC-SC decreases the phase shifts caused by SFOs significantly, which limits the influence range of the interferences.

Fig. 13 shows the BER performance of STBC and STBC-SC when SFO1/SFO2 = 50/-50ppm and SFO1/SFO2 = 70/-30ppm for 16QAM. We see that the STBC cannot work even for SFO1/SFO2 = 50/-50ppm. This is because the distances between constellations are closer than those for QPSK, the spreads of the constellation points caused by SFOs get across the decision boundary. So a lot of decisions are wrong for the subcarriers on the edge, even there is no interference between orthogonal branches. By contrast, STBC-SC can still work, and outperforms the ideal STBC with no SFOs by 3~4dB. When the mean SFO estimation error is 20ppm, the degradation of STBC-SC is smaller than 1.5dB for BER = 4×10^{-4}.

From another point of view, because our SFOs self-cancellation scheme is robust to mean SFO estimation error, it is suitable to the case where the SFOs may change during the transmission of one packet.

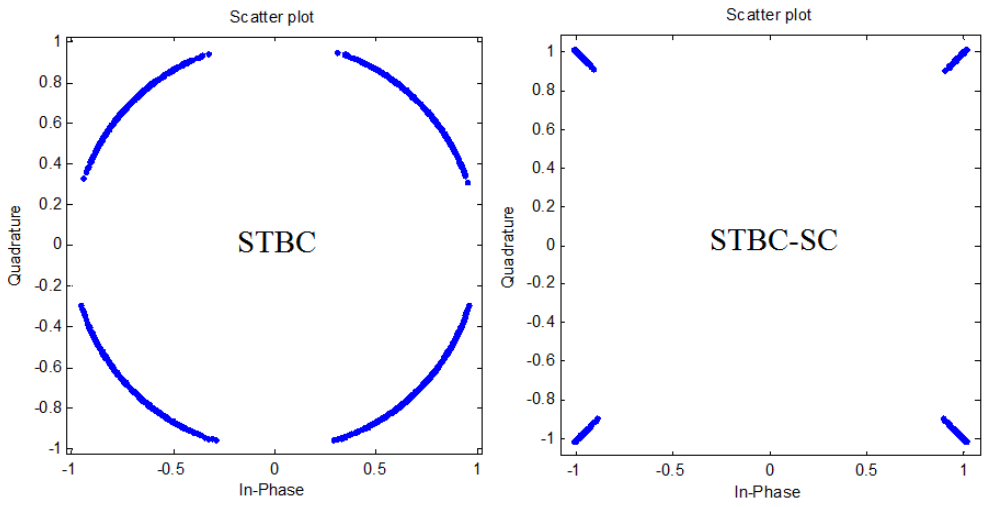

(a) SFO1/SFO2=50/-50ppm

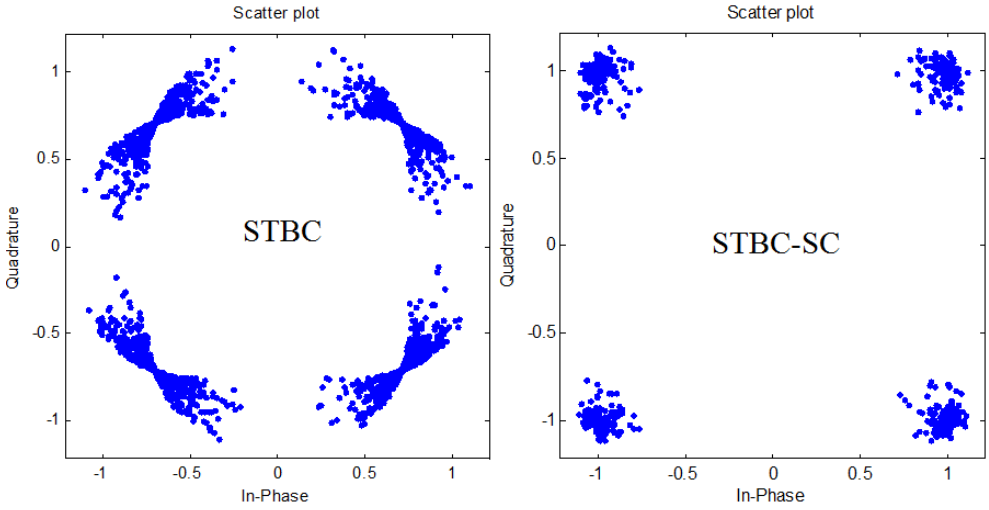

(b) SFO1/SFO2=70/-30ppm

Fig. 11. Constellations for STBC and STBC-SC with no noise

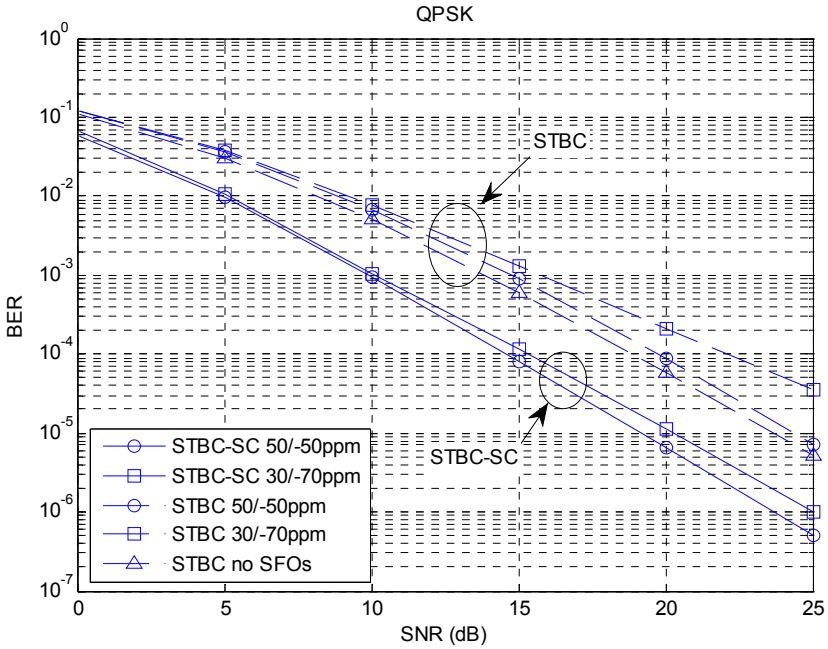

Fig. 12. BER of STBC and STBC-SC (QPSK)

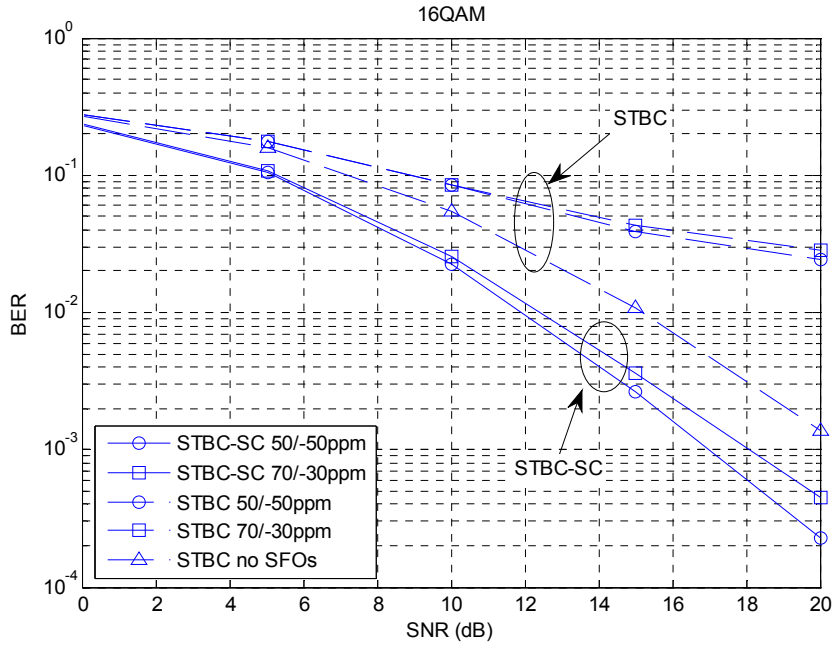

Fig. 13. BER of STBC and STBC-SC (16QAM)

5. Energy efficiency improvement and the price

Because reduced complexity directly leads to improved energy efficiency, in this section, we firstly analyze the complexity reduction brought by the self-cancellation scheme for single SFO relative to the conventional re-sampling method, and then we go to the complexity problem of the self-cancellation scheme for two SFOs in Alamouti coded OFDM based CTs. Finally, the price for the improvement is discussed in the third part.

5.1 Complexity analysis for the self-cancellation for single SFO

Taking the system in Section 4 as an example, if $N = 64$, $N_g = 16$ ($N_s = N + N_g = 80$), and one packet contains 50 OFDM symbols, the total length of one packet is 4000 samples. If the re-sampling is applied to correct a -50ppm SFO, three steps are involved (Crochiere & Rabiner, 1981): firstly, 19999 zeros are filled between each pair of input samples, which process is called interpolation; secondly, the interpolated stream goes through a low-pass filter; finally, the expected output is obtained by extracting every 20000 samples of the filtered stream, which process is called decimation. Although this complex process can be implemented efficiently by a time-varying FIR filter (Crochiere & Rabiner, 1981), because the FIR filter needs to be designed specifically for each estimated SFO, the computation complexity is still too high. For example, if the FIR filter only has 5 taps, then the generation of one sample needs 5 multiplications and 4 additions, so totally 20000 multiplications and 16000 additions are required for the whole packet.

In contrast, if the proposed self-cancellation is applied for the SFO correction, except that SFO estimation is avoided, only 32 addition operations are performed for each OFDM symbol, which means totally 32×50 = 1600 addition operations for the whole packet. We can see the synchronization complexity is reduced by over 99%, which leads to tremendous energy saving.

5.2 Complexity problem for the self-cancellation for two SFOs

As introduced in Section 1, there is no effective correction method for the two SFOs in the OFDM based CTs to our knowledge, so it's not easy to show directly the complexity reduction of the proposed scheme. However, several important facts cannot be ignored. Firstly, we just apply single re-sampling to solve the problem of two SFOs, which cannot even be solved by two re-samplings. Secondly, only single SFO estimation is performed for the purpose of re-sampling, and because our scheme is robust to the SFO estimation error, the mean SFO estimation can be an approximate version with low complexity. Thirdly, if taking the same example in Section 5.1, the complexity of the proposed scheme for two SFOs is only 1% higher than the re-sampling based correction method for single SFO in conventional OFDM systems. Based on these facts, we can say that the proposed self-cancellation scheme is still a low-cost solution for the two SFOs in Alamouti coded OFDM based CT systems.

5.3 The price for low complexity

Although the proposed schemes have low complexity, the bandwidth efficiency is cut down by half in the proposed systems due to the self-cancellation coding. In other words, we

sacrifice the bandwidth efficiency for the energy efficiency. However, due to the diversity gain and array gain we get through the self-cancellation coding, the price is reduced. The simulations in (Gao & Ingram, 2010) shows that, in conventional OFDM system, the BER performance of the SFO self-cancellation scheme even outperforms the ideal OFDM system with on SFO, for the same energy per bit. But by comparing the BER performance of ideal STBC for QPSK (triangle-dashed curve in Fig. 13) and that of the STBC-SC for 16QAM (circle-solid curve in Fig. 14), we find that this advantage diminishes when the self-cancellation is applied in Alamouti coded OFDM based CTs. The reason is that the space-time coding already provides the diversity gain, so the additional improvement brought by the combining in the frequency domain cannot be as obvious as that for conventional OFDM systems.

We want to claim that, although the proposed scheme may require double time for transmitting the same amount of information because of the self-cancellation coding, it actually improve the energy efficiency of the CT system indirectly. CT itself is an energy efficient transmission technology, but the sensitivity to SFOs limits its advantages. The proposed solution to SFOs helps CT getting the best performance with additional diversity gain and array gain, which can be seen as a indirect improvement of the energy efficiency of the system. From another point of view, without a reliable solution to the SFOs problem, it's very possible that the SFOs fail the reception and a retransmission process may be activated, which will cost much more energy.

As introduced in the Section 1, because there are no other effective solutions to the problem of two SFOs in OFDM-based CT systems to our knowledge until now, we can only show the advantages of the proposed solution in terms of energy efficiency in such an indirect way. In future work, the tradeoff between the accuracy of the SFO estimation and the energy consumption should be studied carefully, so that the energy consumption of the proposed solution can be shown explicitly.

6. Summary

OFDM based Alamouti coded cooperative transmission is an efficient transmission technology in sensor networks and cellular networks, but the system is sensitive to SFOs between the transmitters and the receiver. This chapter proposed a simple method to remove the effect of the SFOs, so that the advantages of cooperative transmission can be achieved sufficiently. In this chapter, the SFO self-cancellation scheme for single SFO in conventional OFDM systems is firstly introduced. Then, after analyzing the expression of the STBC decoded symbols, we find that by adjusting the sampling frequency based on the estimated mean SFO, the self-cancellation scheme for single SFO can also work well in 2-branch STBC-OFDM systems. The drawback of this scheme is that the bandwidth efficiency is cut down by half because of the self-cancellation encoding. However, the diversity gain and array gain obtained through the self-cancellation decoding decrease this price. Simulation results show that the proposed scheme removes the phase rotation caused by the two SFOs successfully, which indirectly limits the influence of the interference between STBC branches. Our design outperforms the ideal STBC system with no SFOs, and is robust to the mean SFO estimation error, which implies that our design is suitable to the case where the SFOs may change during the transmission of one packet.

The proposed scheme brought improved energy efficiency. More specifically, when the SFO self-cancellation is applied in conventional OFDM system, the energy efficiency improvement is embedded in both the reduced synchronization complexity and the improved signal transmission efficiency; while, when the self-cancellation scheme is applied in Alamouti coded OFDM based CTs, the energy efficiency improvement is mainly shown by the low-cost synchronization process.

7. Acknowledgment

This work is supported by the National S&T Major Project (2011ZX03003-003-01). The first author also appreciates the support from the Wireless and Mobile Communication Technology R&D Center (WMRC) of Tsinghua University.

8. References

Alamouti, S.M. (1998). A simple transmit diversity technique for wireless communications, *IEEE Journal on Selected Areas in Communications,* Vol. 16, No. 8, (Oct. 1998P, pp. 1451–1458, ISSN 0733-8716.

Commission of the European Communities. (1989). Digital Land Mobile Radio Communications-COST 207. ETSI. 1989.

Crochiere, R.E. & Rabiner, L.R. (1981). Interpolation and decimation of digital signals—A tutorial review, *Proceedings of the IEEE*, Vol. 69, No. 3, (March 1981), pp. 300-331, ISSN 0018-9219.

Fechtel, S. A. (2000). OFDM carrier and sampling frequency synchronization and its performance on stationary and mobile channels, *IEEE Transactions on Consumer Electronics,* Vol. 46, No. 3, (Aug. 2000), pp. 438–441, ISSN 0098-3063.

Gao, Z. & Ingram, M. A. (2010). Self-Cancellation of Sample Frequency Offset in OFDM Systems in the Presence of Carrier Frequency Offset, *Proceedings of the 2010 IEEE 72th Vehicular Technology Conference*, pp. 1-5, ISBN 978-1-4244-3573-9, Ottawa, Canada, Sep. 6-9, 2010.

Heaton, R.; Duncan, S. & Hodson, B. (2001). A Fine Frequency and Fine Sample Clock Estimation Technique for OFDM Systems, *Proceedings of the 2001 IEEE Vehicular Technology Conference*, pp. 678-682, Rhodes, Greece, May 6-9, 2001.

Heiskala, J & Terry, J. (2002). *OFDM Wireless LANs:A Theoretical and Practical Guide*., Sams, ISBN-10: 0672321572, Indianapolis, USA.

Horlin, F. & Bourdoux, A. (2008). *Digital Compensation for Analog Front-Ends: A New Approach to Wireless Transceiver Design*, Wiley, ISBN 978-0-470-51708-6, Chippenham, England.

IEEE (1999), Part 11: Wireless LAN Medium Access Control (MAC) and Physical Layer (PHY) Specifications, *IEEE Std 802.11a-1999*, Sep. 1999.

Kai, S.; Serpedin, E. & Ciblat, P. (2005). Decision-directed fine synchronization in OFDM systems, *IEEE Transactions on Communications*, Vol.53, No.3, (March 2005), pp.408–412, ISSN 0090-6778.

Kim, D. K.; Do, S. H.; Cho, H. B.; Chol, H. J. & Kim, K. B. (1998). A new joint algorithm of symbol timing recovery and sampling clock adjustment for OFDM systems, *IEEE Transactions on Consumer Electronics,* Vol. 44, No. 3, (Aug. 1998), pp. 1142–1149, ISSN 0098-3063.

Kleider, J.E.; Xiaoli Ma & Steenhoek, C. (2009). Distributed Multiple Antenna Carrier and Sampling Frequency Synchronization for OFDM, *Proceeding of IEEE Military Communications Conference, 2009,* pp 1-7, ISBN 978-1-4244-5238-5, Oct. 18-21 2009.

Li, Z. & Xia, X.-G. (2007). A simple Alamouti space-time transmission scheme for asynchronous cooperative systems, *IEEE Signal Processing Letters*, Vol. 14, No. 11, (Nov. 2007), pp. 804-807, ISSN 1070-9908.

Li, Z.; Xia, X.-G. & Lee, M. H. (2010). A Simple Orthogonal Space-Time Coding Scheme for Asynchronous Cooperative Systems for Frequency Selective Fading Channels, *IEEE Transactions on Communications*, Vol. 58, No. 8, (Aug. 2010), pp. 2219–2224, ISSN 0090-6778.

Liu, S.-Y. & Chong, J.-W. (2002). A study of joint tracking algorithms of carrier frequency offset and sampling clock offset for OFDM based WLANs, *Proceeding of IEEE 2002 International Conference on Communications, Circuits and Systems and West Sino Expositions,* pp. 109-113, ISBN 0-7803-7547-5.

Morelli, M. & Moretti, M. (2010). Fine Carrier and Sampling Frequency Synchronization in OFDM systems, *IEEE Transactions of Wireless Communications*, Vol. 9, No. 4, (April 2010), pp. 1514-1524, ISSN 1536-1276.

Morelli, M.; Imbarlina, G. & Moretti, M. (2010). Estimation of Residual Carrier and Sampling Frequency Offsets in OFDM-SDMA Uplink Transmissions, *IEEE Transactions on Wireless Communications*, Vol. 9, No. 2, (Feb. 2010), pp. 734-744, ISSN 1536-1276.

Nee R. & Prasad, R. (2000). *OFDM for Wireless Multimedia Communications,* Artech House, ISBN-10: 0890065306, Boston, USA.

Oberli, C. (2007). ML-based tracking algorithms for MIMO-OFDM, *IEEE Transactions on Wireless Communications*, Vol. 6, No. 7, (July 2007), pp. 2630-2639, ISSN 1536-1276.

Pollet, T. & Peeters, M. (1999). Synchronization with DMT Modulation, *IEEE Communications Magazine*, Vol. 37, No. 4, (April 1999), pp. 80-86, ISSN 0163-6804.

Pollet, T.; Spruyt, P. & Moeneclaey, M. (1994). The BER performance of OFDM systems using non-synchronized sampling, *Proceeding of 1994 IEEE Global Telecommunications Conference* , pp. 253–257, ISBN 0-7803-1820-X, Nov. 28 - Dec. 2 1994.

Sathananthan, K.; Athaudage, C.R.N. & Qiu, B. (2004). A novel ICI cancellation scheme to reduce both frequency offset and IQ imbalance effects in OFDM, *Proceeding of 2004 Ninth International Symposium on Computers and Communications,* pp: 708 – 713, ISBN 0-7803-8623-X

Shafiee, H.; Nourani, B. & Khoshgard, M. (2004). Estimation and Compensation of Frequency Offset in DAC/ADC Clocks in OFDM Systems, *Proceeding of 2004 IEEE International Conference on Communications,* pp. 2397-2401, ISBN 0-7803-8533-0, June 20-24, 2004.

Shin, O. S.; Chan, A. M.; Kung, H. T.; & Tarokh, V. (2007). Design of an OFDM cooperative space-time diversity system, *IEEE Transactions on Vehicular Technology*, Vol. 56, No. 4, July 2007, pp. 2203–2215, ISSN 0018-9545.

Simoens, S.; Buzenac, V. & De Courville, M. (2000). A new method for joint cancellation of clock and carrier frequency offsets in OFDM receivers over frequency selective channels, *Proceedings of the 2000 IEEE Vehicular Technology Conference*, pp. 390-394, ISBN 0-7803-5718-3, Tokyo, Japan, May 15-18, 2000.

Sliskovic, M. (2001). Sampling frequency offset estimation and correction in OFDM systems, *Proceeding of* 2001 *the 8th IEEE International Conference on Electronics, Circuits and Systems, 2001,* pp. 437-440, ISBN 0-7803-7057-0, Sep. 2-5, 2001.

Speth, M.; Fechtel, S.; Fock, G. & Meyr, H. (2001). Optimum receiver design for wireless broadband systems using OFDM —Part II, *IEEE Transactions on Communications*, Vol. 49, No. 4, (Apr. 2001), pp. 571–578, ISSN 0090-6778.

Speth, M.; Fechtel, S.A.; Fock, G. & Meyr, H. (1999). Optimum receiver design for wireless broadband systems using OFDM—Part I, *IEEE Transactions on Communications*, Vol. 47, No. 11, (Nov. 1999), pp. 1668–1677, ISSN 0090-6778.

Tang, S.; Gong, K. & Song, J. Pan, C. & Yang, Z. (2007). Intercarrier interference cancellation with frequency diversity for OFDM systems. *IEEE Transactions on Broadcasting*, Vol. 53, No.1, (March 2007), pp. 132-137, ISSN 0018-9316.

Zhang, W.; Li, Y.; Xia, X.-G.; Ching, P. C. & Letaief, K. B. (2008). Distributed space-frequency coding for cooperative diversity in broadband wireless ad hoc networks, *IEEE Transactions on Wireless Communications*, Vol. 7, No. 3, (Mar 2008), pp. 995-1003, ISSN 1536-1276.

Zhao, Y. & Haggman, S. G. (2001). Intercarrier interference self-cancellation scheme for OFDM mobile communication systems, *IEEE Transactions on Communications*, Vol. 49, No. 7, (Jul. 2001), pp. 1185–1191, ISSN 0090-6778.

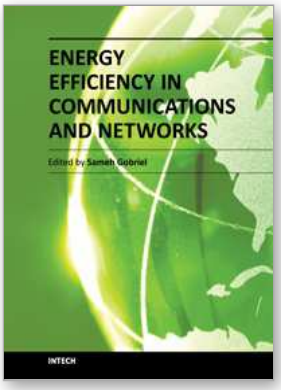

Energy Efficiency in Communications and Networks

Edited by Dr. Sameh Gobriel

ISBN 978-953-51-0482-7
Hard cover, 142 pages
Publisher InTech
Published online 04, April, 2012
Published in print edition April, 2012

The topic of "Energy Efficiency in Communications and Networks" attracts growing attention due to economical and environmental reasons. The amount of power consumed by information and communication technologies (ICT) is rapidly increasing, as well as the energy bill of service providers. According to a number of studies, ICT alone is responsible for a percentage which varies from 2% to 10% of the world power consumption. Thus, driving rising cost and sustainability concerns about the energy footprint of the IT infrastructure. Energy-efficiency is an aspect that until recently was only considered for battery driven devices. Today we see energy-efficiency becoming a pervasive issue that will need to be considered in all technology areas from device technology to systems management. This book is seeking to provide a compilation of novel research contributions on hardware design, architectures, protocols and algorithms that will improve the energy efficiency of communication devices and networks and lead to a more energy proportional technology infrastructure.

How to reference

In order to correctly reference this scholarly work, feel free to copy and paste the following:

Zhen Gao and Mary Ann Ingram (2012). Self-Cancellation of Sampling Frequency Offsets in STBC-OFDM Based Cooperative Transmissions, Energy Efficiency in Communications and Networks, Dr. Sameh Gobriel (Ed.), ISBN: 978-953-51-0482-7, InTech, Available from: http://www.intechopen.com/books/energy-efficiency-in-communications-and-networks/sfos-self-cancellation-in-alamouti-coded-ofdm-based-cooperative-transmission

INTECH
open science | open minds

InTech Europe
University Campus STeP Ri
Slavka Krautzeka 83/A
51000 Rijeka, Croatia
Phone: +385 (51) 770 447
Fax: +385 (51) 686 166
www.intechopen.com

InTech China
Unit 405, Office Block, Hotel Equatorial Shanghai
No.65, Yan An Road (West), Shanghai, 200040, China
中国上海市延安西路65号上海国际贵都大饭店办公楼405单元
Phone: +86-21-62489820
Fax: +86-21-62489821